ELSEVIER

NeuroImage

www.elsevier.com/locate/ynimg
NeuroImage 31 (2006) 1726 – 1740

Spatiotemporal dynamics and connectivity pattern differences between centrally and peripherally presented faces

Lichan Liu and Andreas A. Ioannides*

Laboratory for Human Brain Dynamics, RIKEN Brain Science Institute (BSI), 2-1 Hirosawa, Wakoshi, Saitama, 351-0198, Japan

Received 4 May 2005; revised 26 January 2006; accepted 6 February 2006
Available online 24 March 2006

Most neuroimaging studies on face processing used centrally presented images with a relatively large visual field. Images presented in this way activate widespread striate and extrastriate areas and make it difficult to study spatiotemporal dynamics and connectivity pattern differences from various parts of the visual field. Here we studied magneto-encephalographic responses in humans to centrally and peripherally presented faces for testing the hypothesis that processing of visual stimuli with facial expressions of emotions depends on where the stimuli are presented in the visual field. Using our tomographic and statistical parametric mapping analyses, we identified occipitotemporal areas activated by face stimuli more than by control conditions. V1/V2 activity was significantly stronger for lower than central and upper visual field presentation. Fusiform activity, however, was significantly stronger for central than for peripheral presentation. Both the V1/V2 and fusiform areas activated earlier for peripheral than for central presentation. Fast responses in the fusiform were found at 70–80 ms after image onset, as well as a response at 130–160 ms. For peripheral presentation, contralateral V1/V2 and fusiform activated earlier (10 ms and 23 ms, respectively) and significantly stronger than their ipsilateral counterparts. Mutual information analysis further showed linked activity from bilateral V1/V2 to fusiform for central presentation and from contralateral V1/V2 to fusiform for lower visual field presentation. In the upper visual field, the linkage was from fusiform to V1/V2. Our results showed that face stimuli are processed predominantly in the hemisphere contralateral to the stimulation and demonstrated for the first time early fusiform activation leading V1/V2 activation for upper visual field stimulation.

Keywords: Magnetoencephalography (MEG); Striate cortex; Extrastriate cortex; Fusiform gyrus; Face perception; Connectivity

Introduction

It is well established that visual stimuli presented in one part of the visual field are projected to the contralateral part of the visual cortex such that images presented in the right visual field are projected to the left visual cortex. It is, however, unclear whether stimuli presented in different parts of the visual field are processed differently in extrastriate areas that specialize for processing complex properties of stimuli and whether different connectivity patterns are produced between striate and extrastriate cortices when such complex stimuli are presented to different quadrants. To address these questions, one needs to incorporate three ingredients in the experimental design and analysis. First, one must use stimuli that are known to excite at least one specific extrastriate area well. Second, one must present stimuli at positions in the visual field known to project to specific parts of the visual cortex so that the early entry into the visual system via V1 can be reliably extracted for connectivity analysis. Third, one must use a technique that can provide refined spatial and temporal information about brain activity. The information can then be used in follow-up analysis of spatiotemporal dynamics and connectivity patterns in the brain.

The choice of faces is obvious because many studies have shown that faces are effective stimuli for exciting extrastriate areas. The posterior fusiform gyrus was first associated with cortical face processing from lesion studies on patients with specific recognition deficits of familiar faces (Meadows, 1974; Damasio et al., 1990; Sergent and Poncet, 1990). Neuroimaging studies have shown that extrastriate areas are involved in face processing in normal subjects using techniques such as positron emission tomography (PET) (Sergent et al., 1992; Haxby et al., 1994), functional magnetic resonance imaging (fMRI) (Puce et al., 1995; McCarthy et al., 1997; Kanwisher et al., 1997; Halgren et al., 1999), electroencephalography (EEG) (Allison et al., 1994; Bentin et al., 1996; George et al., 1996) and magnetoencephalography (MEG) (Linkenkaer-Hansen et al., 1998; Halgren et al., 2000). In the present study, we chose the same face stimuli from our earlier MEG study on complex object and face affect recognition that were shown to activate extrastriate areas well (Liu et al., 1999; Ioannides et al., 2000).

Most of the earlier studies mentioned above, including ours, have presented facial images centrally with a relatively large visual field covering both the fovea and parafovea. Central presentation of images activates widespread striate and extrastriate areas. Low order visual areas (V1/V2) corresponding to left–right–upper–lower visual field stimulation are therefore activated by the same

* Corresponding author. Fax: +81 48 467 9731.
E-mail address: ioannides@postman.riken.jp (A.A. Ioannides).
Available online on ScienceDirect (www.sciencedirect.com).

1053-8119/$ - see front matter © 2006 Elsevier Inc. All rights reserved.
doi:10.1016/j.neuroimage.2006.02.009

stimulus, making it difficult to disentangle individual contributions from these low order visual areas and follow each through to map connectivity patterns between striate and extrastriate cortices. Very few neuroimaging studies so far were conducted to study the laterality effects systematically (McCarthy et al., 1999; Levy et al., 2001; Terasaki and Okazaki, 2002; Watanabe et al., 2003; Noesselt et al., 2005). Even in these few studies, only left- or right-hemifield presentation with a small offset (less than 2°) from the center was used (McCarthy et al., 1999; Terasaki and Okazaki, 2002; Watanabe et al., 2003). To clarify spatiotemporal dynamics and connectivity pattern differences from various parts of the visual field, in the present study, we presented face stimuli at the center and four quadrants separately, with larger offsets than previous studies (offset from the center 4.1° horizontally and 2.6° vertically).

To understand the dynamic nature of brain activity and connectivity patterns in humans noninvasively, one needs a technique which provides high temporal resolution. Both EEG and MEG offer the required resolution. Earlier event-related potential (ERP) studies identified a negative component N170 that responds maximally to face stimuli over temporo-parietal regions of the human scalp between 140 and 200 ms after stimulus onset (Bentin et al., 1996; George et al., 1996; Eimer, 1998). This N170 component and its MEG analogue (M170) have been widely accepted as indices of early face processing. Some authors have searched for face sensitivity in the signal of individual MEG sensors and analyzed the timing and properties of such "sensors of interest" (SOIs) (Liu et al., 2002). The N170, M170 and SOIs are only waveforms of individual sensors. These waveforms are useful for identifying the presence of face sensitive activations in the brain in a model-independent way but without further analysis they cannot be attributed to activity in any one brain area. Yet, these EEG and MEG waveforms are often linked directly or indirectly to activity in the fusiform, although there is no direct evidence for a one-to-one correspondence between these waveforms and exclusive fusiform activity. It is nevertheless possible to identify focal activity in specific brain regions from the topography of magnetic fields around the head recorded from full set of MEG sensors covering the whole head using modern MEG hardware. Unlike EEG, MEG is less sensitive to detailed assumptions about the conductivity profile, so it has greater spatial resolution for localizing generators in the brain. Our two recent MEG studies have demonstrated accurate localization at both cortical (Moradi et al., 2003) and sub-cortical (Ioannides et al., 2005) levels. In our earlier MEG studies of brain activations elicited by face stimuli, we have consistently identified fusiform activity during the period of N170 (Liu et al., 1999; Ioannides et al., 2000, 2004), consistent in terms of Talairach coordinates (Talairach and Tournoux, 1988) with what has been called the fusiform face area (FFA) (Kanwisher et al., 1997). In these earlier studies, we identified the same FFA focal area in statistical comparisons between post- and pre-stimulus periods and in comparisons between activations elicited by faces and other stimuli (Ioannides, 2001). Detailed single trial analysis of the same data demonstrated that this FFA activity was always part of activity in a network of areas (Ioannides et al., 2004). In the present study, we used face stimuli from the same set as in our previous studies and analyzed the spatiotemporal dynamics and connectivity patterns when the stimuli were presented in different parts of the visual field. We used the following three strategies to analyze the MEG signal. First, to capture fast responses in the brain, we used a much higher upper filter cut of 200 Hz than most of previous intracranial, ERP and MEG studies on face processing (often as low as 30 Hz and rarely higher than 100 Hz). Second, to identify brain activity in a model-independent way, we used the same tomographic analysis and statistical parametric mapping as in our earlier studies on face processing using both normal (Liu et al., 1999; Streit et al., 1999, 2003; Ioannides, 2001; Ioannides et al., 2000) and schizophrenic subjects (Streit et al., 2001; Ioannides et al., 2004). Third, we used mutual information (Ioannides et al., 2000, 2005) to reveal details of dynamic interchanges between brain regions.

The present study is part of a wider project with overall aim to investigate how visual stimuli with different facial expressions engage cortical and sub-cortical brain areas during a face affect recognition task. A pre-requisite for this goal is to determine whether processing of visual stimuli and especially facial expressions of emotions depends on where the stimulus is presented in the visual field. The work reported in this paper tests the following hypothesis: processing of visual stimuli with facial expressions of emotions depends on where the stimuli are presented in the visual field. We test this hypothesis by addressing three questions: First, how fast is the human fusiform gyrus activated? Second, how do the low order visual (V1/V2) and fusiform areas interact with each other during the face affect recognition task? Third, what is the effect of image presentation position on the activation of V1/V2 and fusiform areas and their interactions? We found that face stimuli are processed predominantly in the hemisphere contralateral to the stimulation and fast responses in human fusiform cortex occur at 70–80 ms after stimulus onset as well as at 130–160 ms. Notably, we demonstrated for the first time early fusiform activation leading V1/V2 activation for upper visual field stimulation. The investigation of face and emotion specificity related to different visual field presentations is now in progress.

Materials and methods

Subjects

Eight healthy right-handed male subjects (mean age 32, range 24–50) volunteered for the MEG experiment. All subjects had normal or corrected-to-normal visual acuity and provided written informed consent. The RIKEN Research Ethical Committee approved the experimental protocol.

Stimuli

Stimuli were chosen from Ekman and Friesen's Pictures of Facial Affect (1976). Five actors (two males) whose expressions were best recognized in posing two facial emotional expressions (happy and fearful) and a neutral face were selected. In each recording run, 15 images (five actors × three emotions) were repeated once and a total of 30 images were randomly presented to subjects. The general visual qualities of each image were digitally reworked to ensure uniformity: a luminance meter was used to adjust the images to natural daylight conditions in rooms (average luminance of 30–40 cd/m^2). Then all the images were mounted into the center of a mid-gray background to ensure uniform figure/ground contrast.

Experimental design

We used a block design for presenting the images in different parts of the visual field: the images appeared at one of the five positions (center or quadrants) on the screen, fixed for each run. Each run consisted of 30 images on a gray background and 15 s of the same background with a fixation cross before and after the 30 images. Hereafter, the image position is referred to as CM (center middle), UL (upper left), UR (upper right), LL (lower left) and LR (lower right). At CM, images subtended 4° and 6° of visual angle horizontally and vertically. In each quadrant (UL, UR, LL, LR), images were 6 × 9° with an eccentricity of 10° (Fig. 1A). Each image was shown for 500 ms and 1 s later an option list of the emotions was shown for 3 s (Fig. 1B). Subjects had to name the emotion verbally as soon as the list appeared. The intertrial interval was randomized between 1.5 and 2.2 s. Three runs for each of the five image positions were recorded. The total recorded runs were therefore 15 (5 positions × 3). The run order was randomized and counter-balanced across subjects. Two subject baseline runs were also recorded, one before and one after the task runs. In these two control runs, subjects were in place with the same luminosity and fixation cross on the screen as in the task runs.

For one subject (subject 1), at the end of the face affect recognition experiment, we also used static circular checkerboards and recorded the MEG signal in the same way as the face stimuli. The checkerboard sizes were radius of 3.0° at the center and 4.5° in the quadrants (same eccentricity as the faces at 10°). The covered visual fields were therefore very similar between checkerboards and faces. There were 5 recording runs, one for each of the five image positions. In each run, 60 trials were recorded with the checkerboard shown for 500 ms and intertrial interval randomized 2.0–2.5 s.

Experimental setup

The stimuli were presented using a XGA LCD projector and back-projected inside the magnetically shielded room using a mirror system onto a screen about 56 cm in front of subjects. An operator recorded subject responses outside the shielded room manually. A photodiode was attached to the screen to mark the exact onset time of each image.

Monitoring eye movements

During the whole recording run, subjects fixated the center of the images for central presentation or a fixation cross at the screen center for peripheral presentation. To achieve this, 1 day before the main experiment, we trained subjects specifically to fixate centrally and not to look at the images directly when they appeared in the quadrants using the same experimental design as in the main experiment but with a different image set (JAFFE database) (Lyons et al., 1998). To monitor subjects' eye movements, we placed one pair of EOG electrodes 1 cm above and below the left eye (vertical movement) and another pair 1 cm lateral to the left and right outer canthus of the eyes (horizontal movement). We recorded and calibrated the EOG signal during training.

MEG signal recording

We recorded MEG signals using a whole head Omega 151-channel system (CTF Systems Inc., Vancouver, BC, Canada) with additional electrodes to monitor subject's artifacts generated from (vertical and horizontal) eye movements and heart function (ECG electrodes, left and right wrists, left and right ankles and lead V2). The MEG signal was recorded in an epoch mode as a 5-s segment beginning from 500 ms before to 4.5 s after each image onset. The recording was made with a low-pass filtering at 200 Hz and sampling at 625 Hz.

Co-registration of MEG and MRI

High-resolution anatomical images of each subject's whole head were taken with a 1.5-T Siemens MRI system. For each subject, T1-weighted MRI images (voxel size of 1 × 1 × 1 mm^3) were collected. Before the MEG experiment, three head coils were attached to the subject's scalp, close to the nasion, left and right pre-auricular points, respectively. The three head coils defined a coil-based coordinate system. During each recording run, subject's

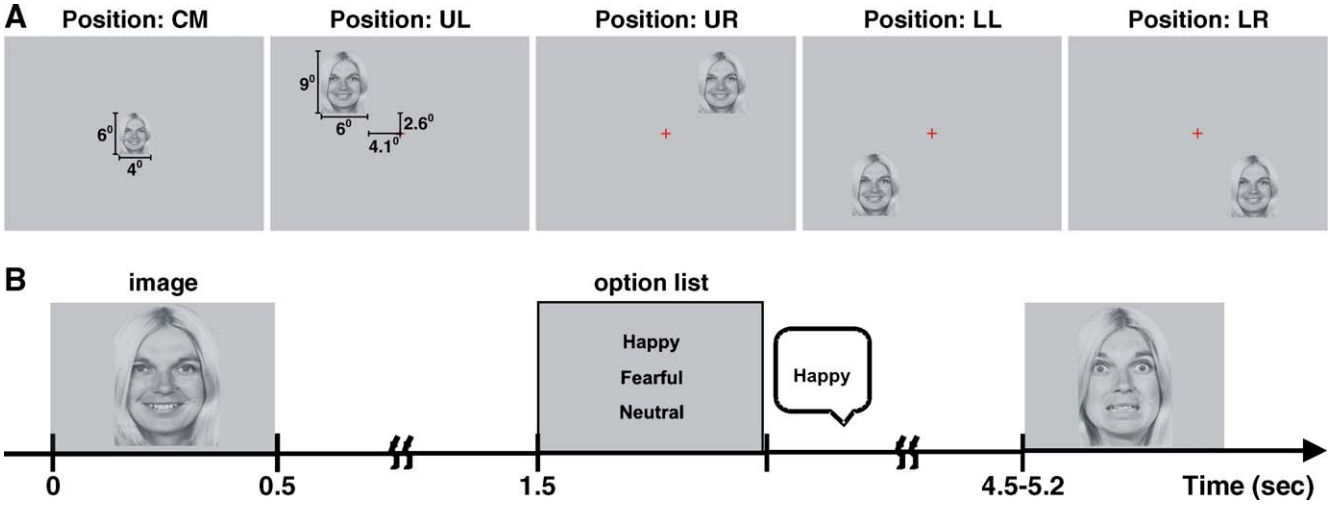

Fig. 1. Experimental setup. (A) The five image presentation positions. (B) The task trial sequence.

head position was monitored with the three head coils. If a subject had moved excessively (4 mm or more) during a run, then the recording for the run was repeated.

Subject's head shape was scanned using a 3D digitizer (Fastrak, Polhemus, Colchester, USA) and a 3D camera system (Vivid 700, Minolta Co. Ltd., Japan). The digitized head shape was fitted on the MRI to get a transformation matrix between coil- and MRI-based coordinate systems using Rapid Form (INUS Co. Ltd., Korea) and dedicated in-house software (Hironaga et al., 2002). The co-registration accuracy was checked manually and matched up within 1–2 mm. If the error of the fit was more than 3 mm, the digitization process was repeated.

MEG signal processing

Off-line, environmental noise was first removed from the MEG signal by forming the third gradient of the magnetic field. The resulting data were filtered using the CTF software in the 3–200 Hz band with notch filters at 50 Hz and its harmonics to eliminate noise generated by the power line. We then extracted trials from each run, 500 ms before to 1 s after image onset. Careful off-line inspection ensured that the extracted MEG signal was free of contamination from subject's mouth movement during speech. Trials with blinks and eye movements (as indicated by the calibrated EOG signals) around image onset (−200 to 500 ms) were rejected manually. On average, about 1–2 trials were rejected in some of the 15 task runs for each subject. For the remaining extracted data, we further removed subject's artifacts such as heart function and eye blinks and movements (not around image onset) using independent component analysis (ICA) (Jahn et al., 1999). Since the purpose of this study was to examine spatial and temporal differences between centrally and peripherally presented facial images, we report here results from ICA-cleaned data averaged on image onset from all images, regardless the emotions shown in the images.

Magnetic field tomography analysis

In recent years, a number of techniques have been proposed for obtaining a map of activations or significant changes in activity throughout the brain. Spatial filtering methods rely on local properties of sensitivity profiles of MEG sensors (lead fields) and the statistics of the MEG signal (usually the covariance matrix) to produce estimates of generators at each grid point separately. In contrast, distributed source methods produce estimates for the local current density at each timeslice from the signal value of each sensor taking into account the local lead field and a global measure. The global measure is the inverse of a matrix whose elements are (weighted) integrals of the overlap of lead fields over the entire source space (Gross and Ioannides, 1999).

Magnetic field tomography (MFT) is a distributed source method, producing probabilistic estimates for the nonsilent primary current density vector $\mathbf{J}(\mathbf{r},t)$ at *each timeslice* of the MEG signal (Ioannides et al., 1990). The MFT algorithm relies on a *nonlinear* solution to the inverse problem, which has optimal stability and sensitivity for localized distributed sources (Taylor et al., 1999).

We have been using the same tomographic analysis (MFT) for our recent studies on face processing in both normal (Liu et al., 1999; Streit et al., 1999, 2003; Ioannides, 2001; Ioannides et al., 2000) and schizophrenic subjects (Streit et al., 2001; Ioannides et al., 2004). Specifically, for each subject, four hemispherical source spaces were defined, each covering the left, right, superior and posterior part of the brain well. Lead fields used for the MFT analysis were computed from a spherical head model for the conductivity of the head, defined separately for each one of the four source spaces. The center of the sphere was chosen by a best fit to the local curvature of the inner surface of the skull below a set of 90 MEG channels. MFT was used to extract brain activity separately from the signal corresponding to the 90 channels selected for each of the four source spaces. The results from the four source spaces were then combined into one large source space covering the entire brain and stored in an $8 \times 8 \times 8$ mm source space grid. The algorithmic steps and mathematical details of the method can be found elsewhere (Ioannides et al., 1990, 1995; Taylor et al., 1999).

For each subject, we applied MFT to the averaged data from the 15 task and 2 control runs, from 200 ms before to 600 ms after image onset at a step of 1.6 ms. The MFT solutions produced probabilistic estimates for the instantaneous current density vector $\mathbf{J}(\mathbf{r},t)$ throughout the *entire* brain every 1.6 ms, capturing time-locked components of activity evoked by the facial images.

Post-MFT statistical parametric mapping analysis

Since the MFT computation was performed independently for each timeslice, we were able to treat the modulus of the current density vector at each timeslice and source space grid point as an independent random variable. We could therefore use statistical analysis to identify brain areas and latency periods when the activity was significantly different between conditions (Liu et al., 1999; Ioannides, 2001).

For each image position (3 runs), we first identified strongly and consistently activated areas by calculating the averaged current density vector smoothed with a moving window of 6.4 ms in a step of 1.6 ms. Then, we investigated if these activations were significantly different between the task and control runs for each subject using statistical analysis. The active distribution at each timeslice was composed of the moduli of the smoothed current density vector from the three task runs at each image position (i.e., 3 elements in each active distribution). Three baseline distributions were made, each corresponding to 120 elements, 60 from each of the two subject baseline runs. The 60 elements were randomly selected from the whole baseline period (−200 to 600 ms, 500 elements). To minimize temporal autocorrelations, we enforced at least 5 ms separation between elements. A t test was made between active and baseline distributions. For each timeslice and image position, we made three separate contrasts, comparing each active distribution with three different baseline distributions. Thus, for each subject, each image location, each timeslice and each source space grid point, we obtained three P values. Each P value included the conservative Bonferroni correction for multiple comparisons across grid points. We chose the least significant comparison (highest P value) as the result for each comparison. This P value corresponded to the confidence level for rejecting the null hypothesis of no significant change of activity in the MFT moduli between task and control runs. The sign of the change was then inspected: a positive P value was retained if the change was positive (i.e., task higher than control), or a negative P value was used to mark decrease of activity. We did not apply correction for multiple comparisons across timeslices because the statistical analysis was already conservative and the results showed statistical significance in sequential latency ranges, which corresponded well

to previous studies with similar stimuli. The statistical significance achieved for each subject was extremely high and would easily survive double Bonferroni correction (for spatial and temporal repetitions of the t test). We used the Bonferroni correction only for the spatial dimension when combining across subjects (see next sub-section) because we were interested in identifying the first timeslice in each of such sequences with high temporal accuracy. We stress that the statistical analysis makes no assumption about the fusiform activity or other regional activity. The loci of significant changes of activity were defined in a model-independent manner: grid point-by-point analysis throughout the entire brain.

Common significantly activated areas across subjects

For each subject, we used post-MFT statistical analysis to obtain maps showing significant changes of activity at each timeslice between each task (e.g., all CM runs) and control condition. These individual maps were then transformed to a common Talairach space. We used the following 3 steps to identify common significantly activated areas across subjects. First, for each subject, positive and negative P values at each source space grid point and timeslice were transformed to new values (Q values) by taking the natural logarithm ($Q = \ln(P)$) and then smoothed separately by a spatial smoothing algorithm based on the sigmoid weight function: $Q_{\text{smoothed}} = \sum_i W_i Q_i / \sum_i W_i$, where $W_i = 1/[1 + \exp[(R_i - c / \alpha)]]$. Q_{smoothed} is the new smoothed value; Q_i is the value at the ith grid point located within a search radius of 1.0 cm from the smoothed point; R_i is the distance between the ith and the smoothed point; c and α are constants specified by the user, defining the shape of the sigmoid weight function. For the present study, we used $c = 0.7$ cm and $\alpha = 0.2$ cm. For each grid point, the highest Q_{smoothed} over the time window $\Delta t = 19.2$ ms was selected, separately for the positive and negative P values. The smoothed P value was then obtained as $P = e^{Q\text{smoothed}}$ with the appropriate sign signifying increase or decrease of activity. Second, across all subjects, for each grid point, percentages of commonality (0–1) were calculated: percent_pos = $N_{\text{pos}} / N_{\text{subjects}}$ and percent_neg = $N_{\text{neg}} / N_{\text{subjects}}$, where $N_{\text{pos}}(N_{\text{neg}})$ is the number of subjects whose significant increase (decrease) in activity was identified at the predefined threshold ($P < 0.05$ in this study). Third, for each grid point we selected the higher absolute value between percent_pos and percent_neg as the output (retaining the appropriate sign).

Regions of interest and activation time courses

We used the foci of common significantly activated areas across subjects to guide the definition of regions of interest (ROIs) for each subject based on functional criteria. First, these common foci were labeled by their anatomical locations (e.g., the fusiform cortex) and then projected back to each subject's MRI based on the Talairach coordinates of the foci. Second, around the projected foci, for each subject, we identified by purely functional criteria the subject specific foci of maximal activity from the averaged current density vector over the MFT solutions for the three task runs at each image position. Third, we defined ROIs as spheres centered on the functionally defined foci with radii of 1.0 cm. Finally, for each of the task and control runs, we calculated an ROI activation time course $M(t)$ from the modulus of the current density vector as a function of time, where $M(t) = \int_{\text{ROI}} \sqrt{\mathbf{J}(\mathbf{r},t)\cdot\mathbf{J}(\mathbf{r},t)}d^3\mathbf{r}$.

Mutual information analysis and influence diagrams

We used mutual information (MI) to examine how activity between different brain areas is linked. MI is computed between two time-lagged time series (Ioannides et al., 2000). The first time series is ROI_1 activation (centered at latency t) while the second time series is ROI_2 activation (centered at latency $t + \Delta t$, where Δt is the delay between ROI_1 and ROI_2 at latency t). In this paper, MI was computed using a window of 48 ms for each time series segment for ROI_1 and ROI_2. We obtained a latency vs. delay contour plot (MI map) by moving the ROI_1 window by 1.6 ms in latency and the ROI_2 window by 1.6 ms in delay. We considered islands of MI values higher than mean plus 5 standard deviations of the pre-stimulus period significant and we interpreted the linkage between the corresponding latency and delay segments as a linked activity between two ROIs at the corresponding latencies (ROI_1 at t and ROI_2 at $t + \Delta t$). The results from the MI maps of each subject were used to identify common MI islands for all subjects. From the common MI islands, we constructed influence diagrams to show more clearly highly significant feed-forward and feedback linkages common to all eight subjects (Ioannides et al., 2005).

Results

Behavioral results

All eight subjects performed the task well above the chance level (33%) regardless of the image presentation positions. Performance was evaluated by the percentage of correct trial (%correct) as a function of image position (UL, UR, CM, LL, LR). Averaged across all eight subjects, the recognition accuracy was best when the images were presented at the center (95.6%), followed by the upper-right (83.6%), upper-left (81.5%), lower-left (80.4%) and lower-right (75.3%). A 3-factor analysis of variance (ANOVA) with image position, subject and facial expression revealed a significant main effect for image position, $F(4,28) = 8.95$, $P < 0.0001$, indicating that response accuracy was affected by where the image was presented. An additional multiple comparison test (Scheffe post hoc test) showed that the performance at the CM position was significantly better than the other four quadrants (UL: $P < 0.02$, UR: $P < 0.04$, LL: $P < 0.006$, LR: $P < 0.00001$), and there was no significant difference in response accuracy between left and right, upper and lower hemifield presentations based on quadrant comparisons (UL vs. UR: $P < 0.99$, LL vs. LR: $P < 0.75$, UL vs. LL: $P < 1.0$, UR vs. LR: $P < 0.29$).

MEG signals

Fig. 2 shows typical MEG signal waveforms from subject 1 as a function of image position. The signal was averaged at the onset of the images from about 30 images in the first of the three runs at one of the five positions. Although MEG signal peak amplitudes were comparable for the five positions, the number of peaks and peak latencies varied with image position. Within 250 ms after image onset, the MEG signal peaked at 40–75 ms, 100–135 ms and 170–210 ms.

Activated brain areas and timing of activation

Using MFT analysis of the MEG signal, we were able to follow neuronal activity across the entire brain millisecond by millisec-

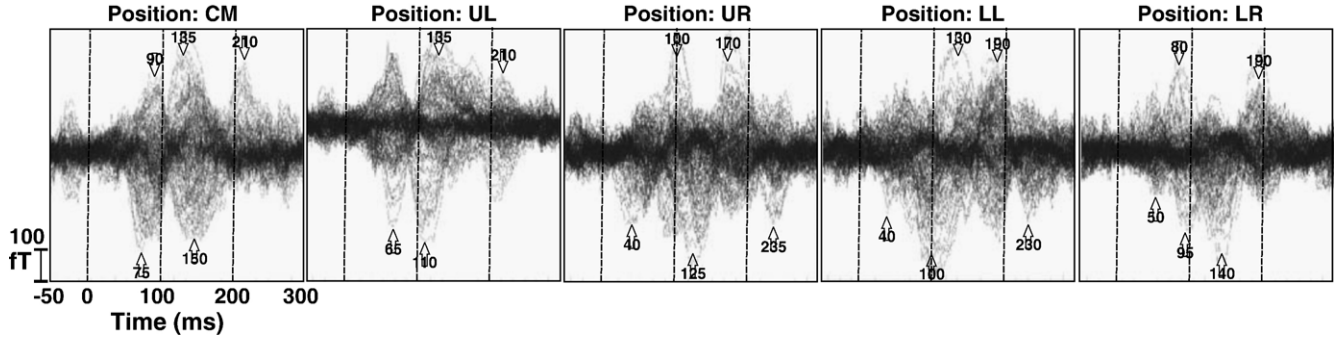

Fig. 2. Averaged MEG signals from subject 1's first run at each of the five image positions (CM, UL, UR, LL, LR). The signal is averaged on image onset over about 30 trials and shown in the same vertical scale. Arrows and numbers highlight peak latencies in the signal traces.

ond. Within 200 ms after image onset, activity was observed in widespread occipital and temporal areas around the calcarine sulcus, occipital gyri (inferior, medial and superior), fusiform gyri (posterior and anterior) and temporal gyri (medial and superior). The activation areas were similar to those that have been reported more responsive to faces than various control stimuli, such as lateral occipital cortex (Gauthier et al., 2000) and posterior superior temporal sulcus (Halgren et al., 1999). Our data show that face stimuli activated a wide network of areas in ventral temporal cortex as reported by others (Haxby et al., 2001) and in our earlier studies (Ioannides et al., 2004). Nevertheless, in this paper, we focus on two areas, the first around the calcarine sulcus (V1/V2) and the second in the posterior fusiform gyri (FG) that showed the most robust difference in activity between faces and objects in our previous MEG studies (Liu et al., 1999; Ioannides et al., 2000, 2004) and other fMRI studies (Kanwisher et al., 1997; Halgren et al., 1999). Restricting the analysis only to two areas on each hemisphere, allowed us to study in detail when the V1/V2 and FG ROIs activated and how they interacted with each other in time when the images were presented at different positions. Table 1 lists the Talairach coordinates for the V1/V2 and FG ROIs. Note that V1/V2 ROI was defined differently for the five image positions, providing results that agree with the well-studied retinotopic organization in the visual system. For central presentation, four V1/V2 ROIs were defined, covering the activated left, right, dorsal and ventral parts of the calcarine sulcus at the pole of the occipital

Table 1
Talairach coordinates x, y, z (mean ± SD) in mm for V1/V2 and FG ROIs

Position	CM	UL	UR	LL	LR
V1/V2	Left-dorsal: −9 ± 2, −84 ± 6, 7 ± 7 Left-ventral: −9 ± 2, −83 ± 3, −7 ± 4 Right-dorsal: 11 ± 2, −84 ± 4, 10 ± 7 Right-ventral: 11 ± 2, −83 ± 4, −5 ± 7	I: −10 ± 2, −81 ± 4, −4 ± 4 C: 11 ± 2, −69 ± 5, 2 ± 7	I: 11 ± 2, −69 ± 5, 2 ± 7 C: −10 ± 2, −81 ± 4, −4 ± 4	I: −10 ± 2, −81 ± 5, 9 ± 6 C: 11 ± 2, −76 ± 3, 16 ± 5	I: 11 ± 2, −76 ± 3, 16 ± 5 C: −10 ± 2, −81 ± 5, 9 ± 6
FG	Left-FG: −32 ± 2, −57 ± 4, −8 ± 4 Right-FG: 33 ± 3, −56 ± 7, −9 ± 5	I: LFG C: RFG	I: RFG C: LFG	I: LFG C: RFG	I: RFG C: LFG
FG1	Left-FG: −35, −49, −11 Right-FG: 29, −58, −19	1 subject in 2 tasks: object recognition and face affect recognition, same face stimuli used in present study, MEG signal recorded with another whole head MEG system (Liu et al. 1999; Ioannides et al. 2000)			
FG2	Left-FG: −39, −50, −16 Right-FG: 32, −46, −9	Same as FG1 study except using another set of 4 healthy individuals and 4 schizophrenia patients (Ioannides et al. 2004)			
Fusiform face area (FFA)	Left-FG: −35, −63, −10 Right-FG: 40, −55, −10	fMRI study (Kanwisher et al., 1997)			
Posterior fusiform gyrus	Left-FG: −42, −58, −18 Right-FG: 37, −52, −17	fMRI study (Halgren et al., 1999)			

The V1/V2 ROI is defined differently for the five image positions (CM, UL, UR, LL, LR): for central presentation, four V1/V2 ROIs were defined. For peripheral presentation, one contralateral V1/V2 ROI was defined; for comparison, ipsilateral V1/V2 ROIs were mirrored from the definition of other hemispheric presentation. The FG ROI definition is the same for all five positions. I (C): ipsilateral (contralateral) hemisphere relative to image position. For reference, the FG ROI definition from our earlier MEG and other fMRI studies was also listed.

lobe. For peripheral presentation, one V1/V2 ROI was defined for the contralateral part of the calcarine sulcus relative to image position (e.g., for UL, the right ventral part of the calcarine). For comparison, ipsilateral V1/V2 ROIs were also quoted; these were mirrored from the definition of other hemispheric presentation (e.g., for UL, ipsilateral V1/V2 ROI was the left ventral part of the calcarine, defined from the UR presentation). Hereafter, contralateral and ipsilateral ROIs are quoted in relation to the image position. As for the FG ROI, our statistical analysis revealed that the activated FG area was similar in location (within a radius of 1.0 cm) for face stimuli presented centrally and peripherally, so we used the same left and right FG ROIs for all five positions. As shown in Table 1, the FG ROI locations matched with those reported in our earlier MEG studies on face processing (Liu et al., 1999; Ioannides et al., 2000) and the FFA reported for face-selective responses by other fMRI studies (Kanwisher et al., 1997; Halgren et al., 1999).

Figs. 3A–H show the first significant change of activity ($P < 0.0001$) around right FG for each subject, obtained from the contrast between centrally presented images in task runs and a blank screen in control runs. The figures show that, while the significant change of activity differed in time for the eight subjects (58–94 ms), the activation area was similar in location. These individual significant maps were then transferred to the common Talairach space, as shown in Fig. 3I, superimposed on the structural MRI from subject 1. Fig. 3I shows the common significantly activated area (red blob), obtained from a search radius of 1.0 cm around the right FG area across all eight subjects, with a search window of 19.2 ms at 72 ms, and again at 162 ms.

Fig. 4A shows a typical example of the right FG ROI definition. The ROI, shown as a blue circle, was defined from the maximal activity of the averaged current density vector (smoothed with a moving window of 6.4 ms in a step of 1.6 ms) over the MFT solutions for the three CM runs. Fig. 4B shows the right FG ROI activation time courses for the three CM runs and the two control runs from subject 1. Right FG activation was much stronger in the task than in the control runs, with peaked activity at 85, 140 and 235 ms. This activation pattern was highly reproducible across the three CM runs, which were recorded at different times during the experiment (maximum of 3 h apart). When images were presented in periphery (Fig. 4C), the right FG area activated earlier and stronger for the left-hemi field presentation (UL and LL,

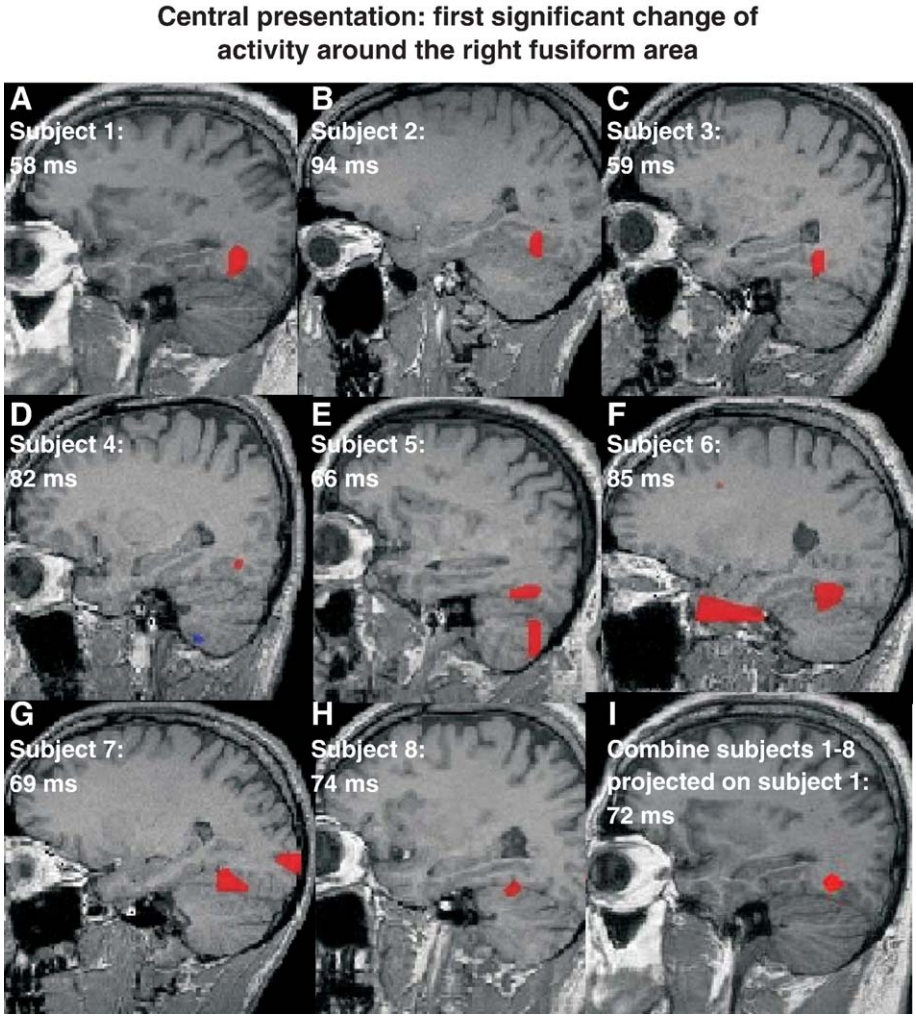

Fig. 3. Statistical maps showing first significant change of activity ($P < 0.0001$) around the right fusiform area for centrally presented images, for each of the eight subjects (A–H) at the printed latency. After transformation of individual maps (A–H) into a common Talairach space, panel I shows the common significantly activated area, obtained from a search radius of 1.0 cm around the right FG area across all eight subjects, with a search window of 19.2 ms at 72 ms.

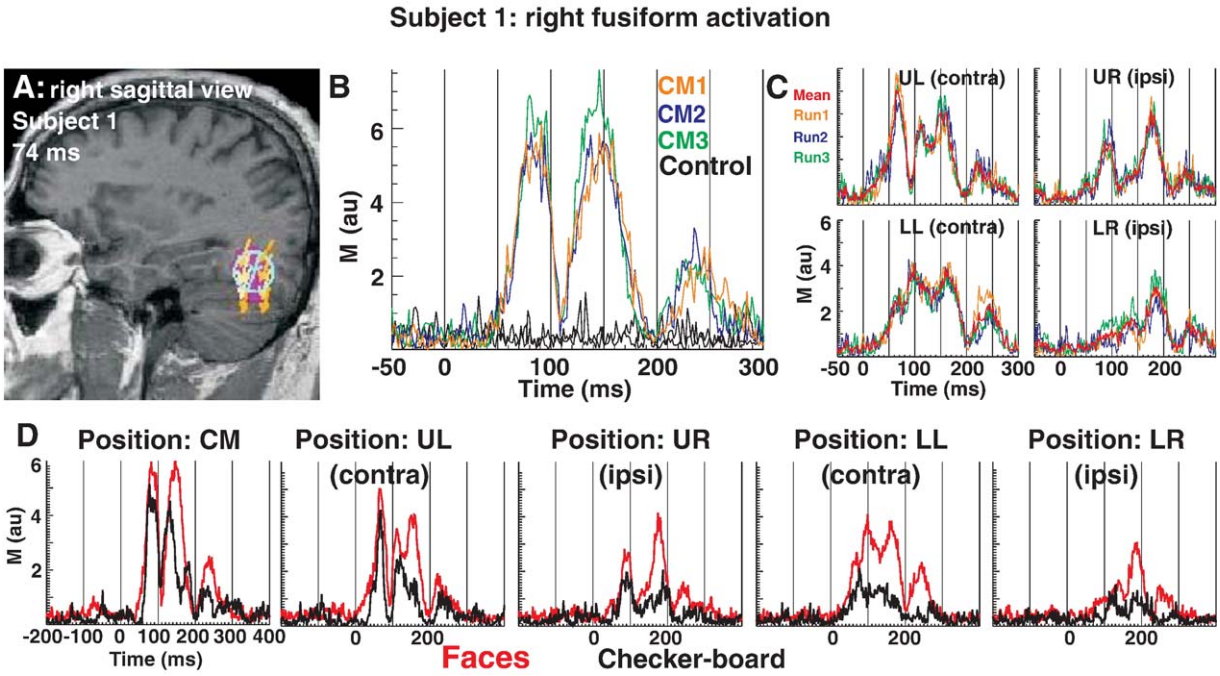

Fig. 4. ROI definition and activation time courses for subject 1's right fusiform area. (A) ROI (blue circle) definition based on the maximal activity of the averaged current density vector (pink blob and small yellow arrows) over the MFT solutions for the three CM runs at 74 ms. (B) ROI activation time courses for the three CM runs and two control runs. (C) Same as panel B except for images presented to one of the four quadrants (UL, UR, LL, LR). Contra (Ipsi): hemi-field presentation contralateral (ipsilateral) to the right FG area. Thin and thick red curves represent the three task runs in each quadrant and the corresponding mean, respectively. (D) Comparison of the right fusiform activation between faces (red) and checkerboards (black) when images were presented to one of the five positions. The red curve is averaged from the three task runs at each position, same as in panel C. The curves in panels C and D are shown in the same vertical scale.

contralateral to the right FG) than for the right-hemi field presentation (UR and LR, ipsilateral to the right FG). Again, the activation profile for each image position was highly reproducible across their respective three repetition runs. For this subject, we also recorded MEG signals for checkerboards presented to one of the five positions. These signals were recorded and processed in the same way as the faces. Fig. 4D compares the right FG activation between faces (averaged over 3 runs; red curves) and checkerboards (black curves) at each position. The figure shows similar activation profiles between the two types of stimuli, but the activation strength was consistently stronger for faces than for checkerboards, especially at later latencies peaked at 140 ms and 235 ms.

Fig. 5 compares V1/V2 ROI activation time courses for images presented to the five positions. For each ROI at each position, the grand averaged activation curve was computed by averaging the individual activation time course from each of the eight subjects. Table 2 lists mean and standard deviation of peak latency (ms) and amplitude (au) from the time courses. Information for two peaks were tabulated, one for the first peak within 100 ms after image onset, the other for the biggest peak within 300 ms. The first peak latency for peripheral presentation (66–80 ms) was earlier than for central presentation (67–88 ms) but this difference did not reach a significant level ($P < 0.15$, ANOVA on first peak latency). The biggest peak latency for central and peripheral presentation ranged from 97–117 ms and 89–136 ms, respectively (only contralateral V1/V2 ROI was considered here for comparison because of much weaker ipsilateral ROI activity). As for the peak amplitude, central presentation activated stronger in the left than right hemisphere ($P < 0.0001$, ANOVA on biggest peak amplitude, mean 4.8 vs. 3.5 au). Peripheral presentation activated the contralateral V1/V2 ROI earlier and significantly stronger than the ipsilateral counterpart area ($P < 0.12$, ANOVA on biggest peak latency, mean 116 vs. 126 ms; and $P < 0.0001$, ANOVA on biggest peak amplitude, mean 4.7 vs. 3.0 au). Lower visual field stimulation activated significantly stronger V1/V2 activity than both central and upper visual field stimulation ($P < 0.0001$, ANOVA on biggest peak amplitude, mean 5.9 vs. 4.1 vs. 3.5 au).

As for the FG activity, Fig. 6 shows the ROI time courses and Table 3 lists the peak latencies and amplitudes. For central presentation, left and right FG showed similar activation patterns (peaked at about 80 and 130 ms), but with stronger activation in the right ($P < 0.09$, ANOVA on biggest peak amplitude, mean 5.6 vs. 4.6 au). For peripheral presentation, contralateral FG activated significantly both earlier and stronger than ipsilateral FG ($P < 0.0001$, ANOVA on biggest peak latency and amplitude, mean 131 vs. 154 ms, mean 3.7 vs. 2.8 au). FG ROI activation was significantly stronger for central than for peripheral presentation ($P < 0.0001$, ANOVA on biggest peak amplitude, mean 5.1 vs. 3.7 au), but the first peak latency was significantly shorter for peripheral than for central presentation ($P < 0.05$, ANOVA on first peak latency, mean 71 vs. 79 ms).

Interactions between V1/V2 and FG areas

The MI was first computed separately for each subject, image position and pair of ROIs. Each MI computation used a pair of 48 ms long windows of ROI activation. The MI map was computed by moving the ROI_1 window (−50 to 100 ms) by 1.6 ms in latency and the ROI_2 window (−100 to 150 ms) by 1.6 ms in delay (i.e.,

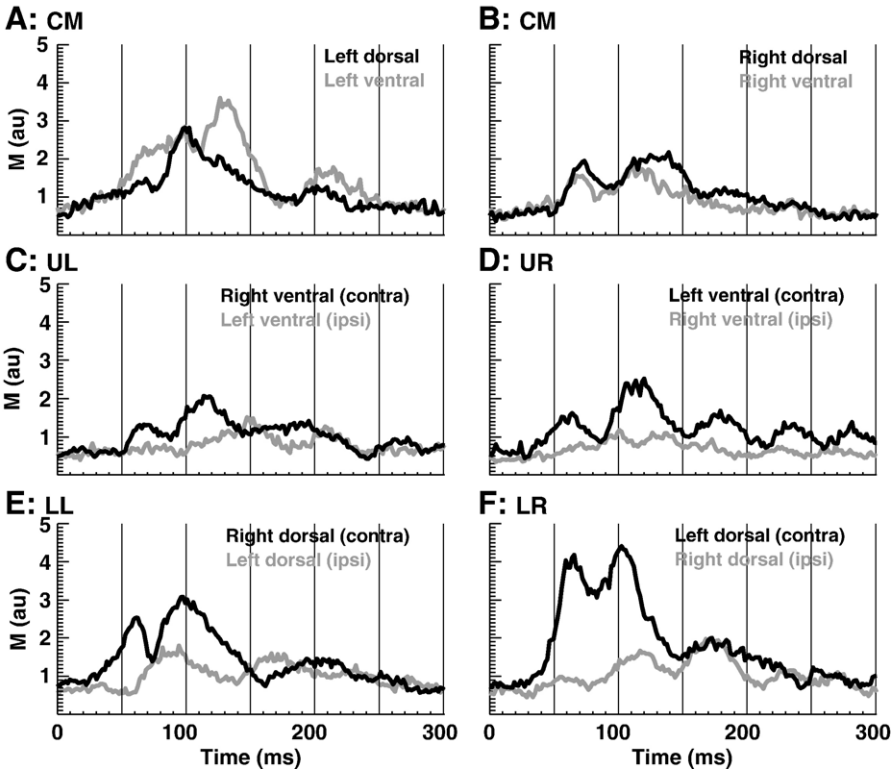

Fig. 5. V1/V2 ROI activation time courses for images presented to the five positions: CM (A,B), UL (C), UR (D), LL (E) and LR (F). For central presentation (A,B), four ROIs were defined and corresponded to the activated dorsal (back), ventral (gray), left (A) and right (B) part of the calcarine sulcus. For peripheral presentation (C–F), one ROI was defined for the contralateral part of the calcarine sulcus relative to image position, and its time course is shown in black. For comparison, time courses for ipsilateral ROIs (mirrored from the definition of other hemispheric presentation) are also shown as gray curves. All panels are shown in the same horizontal and vertical scales.

the delay Δt between ROI_1 and ROI_2 was from −50 to 50 ms). Then the MI map for each subject was normalized to 1.0 and thresholded to mean plus 5 standard deviations of the pre-stimulus period. Finally, the MI maps of each image position and pair of ROIs for different subjects were combined by superimposing all the maps at a threshold of 0.6. The resulting MI maps therefore corresponded to common significant MI values across subjects for each pair of ROI and each image position. Next, we constructed influence diagrams from these common MI maps to show the first significant MI link between pairs of ROIs. Influence diagrams are displayed with ROIs arranged in successive rows with arrows defining linkages between two ROIs. The horizontal axis of the

Table 2
Mean and standard deviation of first peak (0–100 ms) and biggest peak (0–300 ms) latency (ms) and amplitude (au) from the V1/V2 ROI activation time courses

Position	CM	UL	UR	LL	LR
First peak latency (0–100 ms)	L-dorsal: 88.1 ± 13.2 L-ventral: 77.1 ± 20.7 R-dorsal: 73.8 ± 15.5 R-ventral: 66.9 ± 23.3	I: C: 75.6 ± 28.1	I: C: 66.4 ± 26.6	I: C: 73.7 ± 16.3	I: C: 80.1 ± 15.8
First peak amplitude (au)	L-dorsal: 3.3 ± 1.5 L-ventral: 4.5 ± 1.2 R-dorsal: 2.9 ± 0.8 R-ventral: 2.8 ± 1.1	I: C: 2.5 ± 1.0	I: C: 2.9 ± 1.6	I: C: 4.3 ± 2.1	I: C: 6.5 ± 3.1
Peak latency (0–300 ms)	L-dorsal: 116.3 ± 26.4 L-ventral: 117.1 ± 29.2 R-dorsal: 114.1 ± 24.7 R-ventral: 97.3 ± 31.2	I: 136.6 ± 28.4 C: 133.7 ± 42.8	I: 129.1 ± 36.5 C: 135.5 ± 39.0	I: 118.1 ± 45.2 C: 107.5 ± 39.1	I: 144.6 ± 38.5 C: 89.1 ± 29.7
Peak amplitude (au)	L-dorsal: 4.2 ± 1.6 L-ventral: 5.4 ± 1.8 R-dorsal: 3.6 ± 0.8 R-ventral: 3.4 ± 0.9	I: 3.0 ± 1.3 C: 3.3 ± 0.9	I: 2.1 ± 0.9 C: 3.8 ± 1.7	I: 3.6 ± 0.8 C: 4.8 ± 1.8	I: 3.4 ± 1.1 C: 6.9 ± 2.8

I (C): ipsilateral (contralateral) V1/V2 ROI relative to image position. Because of weak activity in ipsilateral V1/V2 ROI, information for the first peak is not listed.

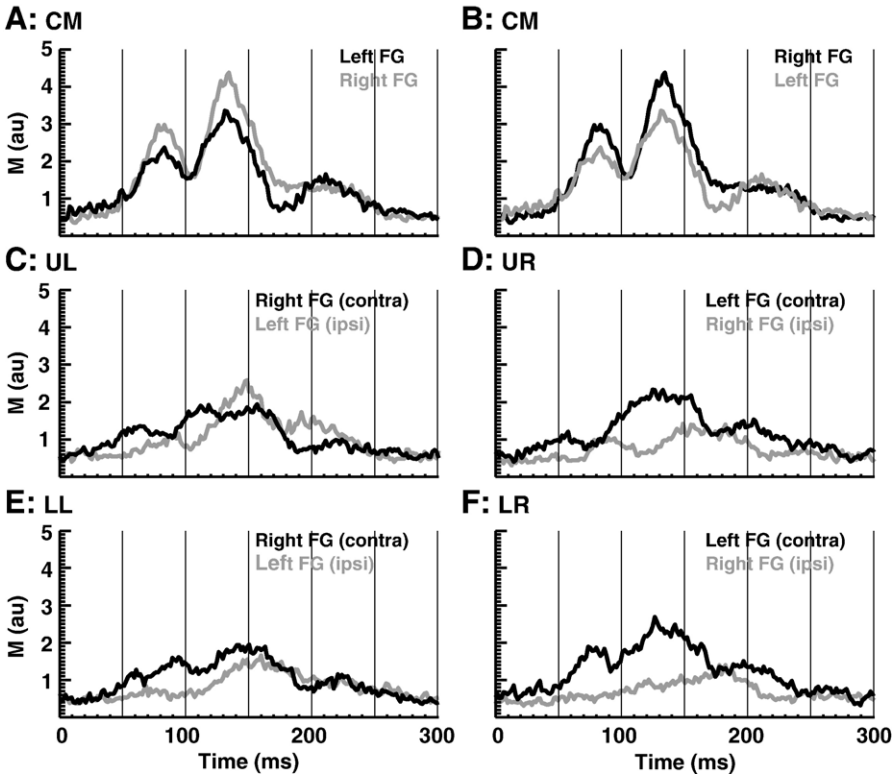

Fig. 6. FG ROI activation time courses for images presented to the five positions with the same layout and scales as in Fig. 5. Left and right FG ROIs were defined for all five positions. Panels A,B for central and panels C–F for peripheral presentation.

diagram shows time flowing from left to right (−100 to 150 ms) with the origin (t = 0) corresponding to image onset. The mutual information is strongly affected by features in regional activations that typically last for 20–30 ms. These typical features influence the MI computation even if a jitter of 10–20 ms is present, because the MI computation uses windows of 48 ms. Accordingly, an uncertainty of at least 10 ms should be allowed for latency (t) in the influence diagram. The arrow direction is defined by the time order of activation: it points from the area activated first to the area activated next. The heavy horizontal black line in each ROI band defines for how long the link activity persists for each linkage that the ROI participates. A pure unidirectional link corresponds to a link where the durations in the source and destination ROIs have no latency overlap.

Fig. 7 shows the influence diagrams for central (A–B) and peripheral (C–D) presentation. Fig. 7A shows how V1/V2 (ROI_1) and FG (ROI_2) on the same hemisphere interacted: the linkage was initiated from V1/V2 to FG, soon followed by a feedback connection from FG to dorsal V1/V2 (red and blue arrows). The linkage was stronger (thicker arrows) between right V1/V2 and right FG (blue and orange arrows) than that between left V1/V2 and left FG (red and green arrows). Fig. 7B shows bi-directional interactions between right (ROI_1) and left (ROI_2) FG. Fig. 7C shows the interactions for V1/V2 (ROI_1)

Table 3
Mean and standard deviation of first peak (0–100 ms) and biggest peak (0–300 ms) latency (ms) and amplitude (au) from the FG ROI activation time courses

Position	CM	UL	UR	LL	LR
First peak latency (0–100 ms)	L-FG: 74.7 ± 22.6 R-FG: 83.7 ± 6.9	I: C: 70.5 ± 23.1	I: C: 69.6 ± 29.1	I: C: 77.7 ± 19.4	I: C: 75.3 ± 19.8
First peak amplitude (au)	L-FG: 3.4 ± 1.7 R-FG: 3.8 ± 1.3	I: C: 3.0 ± 1.7	I: C: 2.3 ± 0.7	I: C: 2.6 ± 0.9	I: C: 3.0 ± 1.5
Peak latency (0–300 ms)	L-FG: 125.1 ± 16.6 R-FG: 131.2 ± 19.5	I: 154.4 ± 18.6 C: 126.6 ± 36.5	I: 154.4 ± 28.4 C: 138.1 ± 19.7	I: 155.2 ± 18.6 C: 130.7 ± 25.1	I: 157.3 ± 27.7 C: 132.5 ± 23.5
Peak amplitude (0–300 ms)	L-FG: 4.6 ± 2.2 R-FG: 5.6 ± 2.1	I: 3.5 ± 1.5 C: 3.8 ± 1.6	I: 2.7 ± 0.9 C: 3.6 ± 1.0	I: 2.5 ± 0.9 C: 3.4 ± 0.8	I: 2.6 ± 0.6 C: 4.1 ± 1.5

I (C): ipsilateral (contralateral) FG ROI relative to image position. Because of weak activity in ipsilateral FG ROI, information for the first peak is not listed.

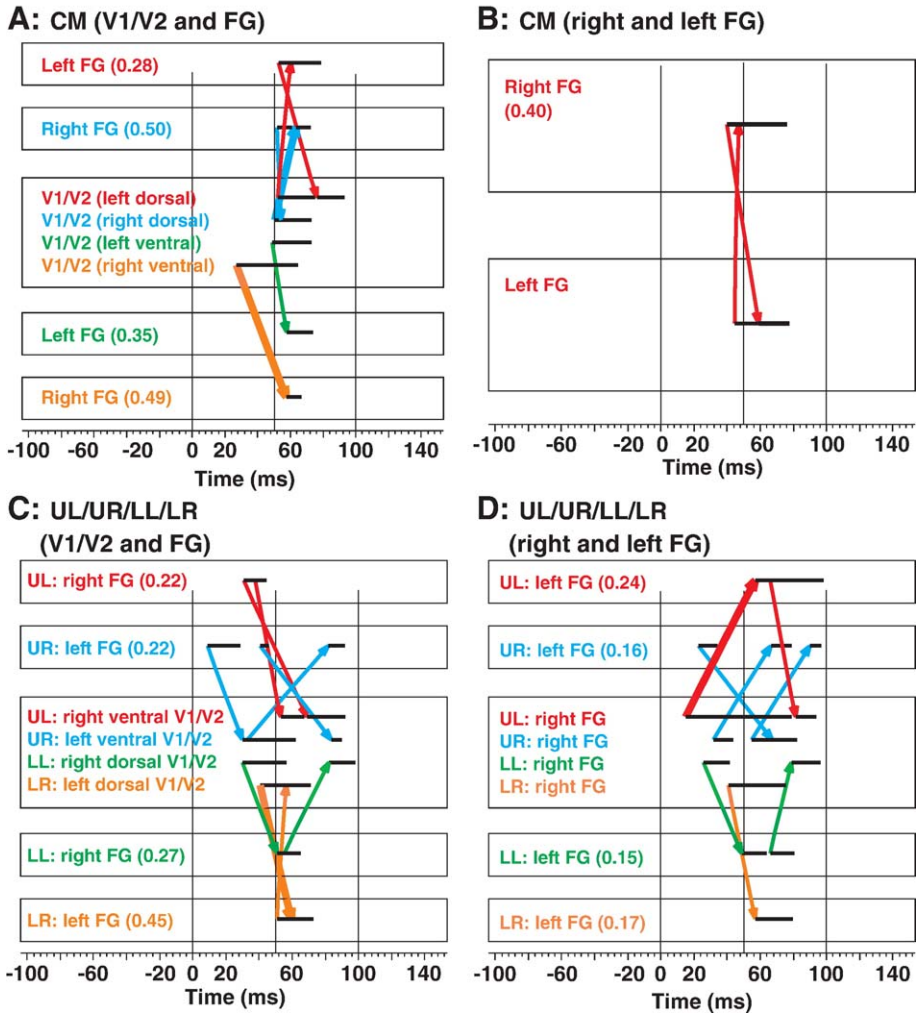

Fig. 7. Influence diagrams for linked activity between V1/V2 and FG common to all eight subjects. ROIs are arranged in successive rows and time flows from left to right with arrows pointing from the first to the second activated area. ROI labels are also printed inside each rows with the numbers denoting the maximum linkage strength between ROI_1 (−50 to 100 ms) and ROI_2 (−100 to 150 ms). Panels A,B for central presentation: (A) linkages between the four V1/V2 ROIs (ROI_1) and FG (ROI_2) on the same hemisphere and (B) linked activity between the right and left FG. (C,D) for peripheral presentation: (C) interactions between contralateral V1/V2 and FG and (D) right and left FG interactions. Heavy arrows denote the strongest linkage in each panel.

and FG (ROI_2) on the contralateral side of the image position. When images were presented in the upper visual field (UL and UR, red and blue arrows), the linkage was from FG to V1/V2, unidirectional for UL and a bi-directional sequence for UR. In contrast, when images were presented in the lower visual field (LL and LR, green and orange arrows), the linkage was first from V1/V2 to FG, soon followed by a feedback link from FG to V1/V2. Among the four quadrant presentations, LR had the strongest linkage (between left V1/V2 and left FG). Fig. 7D shows the interaction between right (ROI_1) and left (ROI_2) FG. The first linkage was from right to left FG except for UR presentation (blue arrow), in which case there was a brief unidirectional link first from left (contralateral to image position) to right FG, and then an independent linkage a few milliseconds later from right (ipsilateral) to the left FG. Feedback connections were also seen from left to right FG for UL and LL (red and green). The linkage between right and left FG for UL was stronger than those for the other 3 quadrant presentations.

Discussion

Scope of the present study

The present study is part of a wider project with an overall goal to use MEG to map the spatiotemporal evolution of activity associated with facial affect recognition. Previous work has identified the key brain areas involved, such as the fusiform cortex (Kanwisher et al., 1997; Liu et al., 1999; Halgren et al., 2000; Ioannides et al., 2000). There was a hint in our earlier studies that early responses (i.e., the first 200 ms after stimulus onset) could strongly depend on where stimuli were presented. The scope of this study was therefore limited to test the hypothesis that processing of facial stimuli in an emotion recognition task depends on where the stimuli were presented in the visual field. The results supported the hypothesis and revealed a rather complex and dynamic relationship between the V1/V2 and FG activity and the location of the stimuli. These results point to new questions that we will discuss after we summarize the results of the present study.

Task performance

In this MEG study, we examined the spatial and temporal differences between centrally and peripherally presented facial images. We used two measures to make the comparison feasible. First, using another set of images, subjects were trained to fixate at the center regardless of image presentation position 1 day before. On the experiment day, all subjects could perform the task without difficulty while maintaining central fixation as confirmed by the EOG recording: 1–2 trials were typically rejected in some runs containing 30 trials due to subject's eye movements. Second, although human ability to perceive spatial stimuli declines with increasing eccentricity, by applying adequate stimulus magnification, one is capable of detecting geometric changes in complex images such as faces equally at the fovea and in the periphery (Rovamo et al., 1997). In this work, we used image size of 4 × 6° for central and 6 × 9° with eccentricity 10° for peripheral presentation. Our behavioral result showed that the performance accuracy was well above the chance level (33%), with 96% and 75–84% correct for central and peripheral presentation, respectively.

The performance was significantly better for central presentation maybe because we generally fix our eyes on faces directly and such daily experience may lead to a center field bias for the face selective cortex (Levy et al., 2001). Alternatively, the size ratio of 1.5 between peripheral and central presentation is slightly lower than the recommend value of 1.7 to 2.5 for performance in the periphery to be maintained at the foveal level (Melmoth et al., 2000).

Fast responses in the fusiform cortex

Earlier ERP studies identified the N170 component as the index of early face processing (Bentin et al., 1996; George et al., 1996; Eimer, 1998), but this does not imply a one-to-one relationship between N170 and fusiform activation. In our earlier MEG study (Liu et al., 1999), using an object recognition task in which we presented centrally the same face stimuli as in the current study together with other 5 object categories (horse faces, birds, flowers chairs and lorries), for faces only, we also observed early peak activity in the fusiform bilaterally (left: 55 ms, right: 75 ms), and the activation strength of this early activity was about one-third in the left and half in the right as compared to later peak activity (left: 148 ms, right: 138 ms). Since our earlier study was a detailed single trial analysis from one subject, we could only make a comment on the fast response in the fusiform.

In the present study, we identified activity in the fusiform gyri directly, at locations similar to those that have been reported for face-selective responses by other studies using fMRI (Kanwisher et al., 1997; Halgren et al., 1999) and those in our earlier studies using the same face stimuli and images of other objects (Liu et al., 1999; Ioannides et al., 2000, 2004). In the present study, we found fast responses in the fusiform at 70–80 ms after image onset (Fig. 6 and Table 3). These latencies are considerably earlier than 170 ms—the latencies which have been attributed to the FG activation. Two possible explanations can be given. First, we used a smaller image size than most of previous EEG/MEG studies. For example, visual angle of centrally presented faces was about 10 × 8° in Halgren et al. (2000) and 9 × 11° in Itier and Taylor (2004). Using larger stimulus size may increase the signal strength and thus may yield better signal-to-noise ratio in the recorded signal, but the excitation of a wider V1/V2 area may also cause large-scale cancellations in FG: if as we have shown, presentation of a stimulus in different parts of the visual field produces V1/V2 activations at significantly different latencies (even within the first 100 ms), then the brief and jittery nature of these activations may lead to a weakly time-locked signal and smeared the early activation in FG and thus difficult to detect and to localize. Second, we filtered the MEG signal over a wider band allowing higher frequencies to survive. In the present study, the upper filter cut was 200 Hz, which was quite different from those used in earlier studies. For example, in recent MEG studies, Linkenkaer-Hansen et al. (1998) used 30 Hz, Watanabe et al. (2003) used 50 Hz and Halgren et al. (2000) used 90 Hz. With such a large filter difference, it is perhaps not surprising that earlier components (fast responses) were not detected in these earlier studies. The choice of a low upper filter cut may be necessary in intracranial studies because these studies were performed on epilepsy patients where transient high-frequency abnormalities were present (Allison et al., 1999; McCarthy et al., 1999). The reason for a low upper filter cut in early ERP/MEG studies using healthy subjects was to obtain "clean" and smooth signals. With modern MEG (and EEG) hardware this is unnecessary as it eliminates information. For each subject, regional activations are highly reproducible (Figs. 4B–C). The high frequency activity the low frequency activity does not survive averaging well while does not always lead to a clear dipolar pattern as many areas may be simultaneously active. Thus, it is not reproducible accurately enough across subjects to survive grand-averaging (Figs. 5 and 6). However, for individual subject, FG showed high frequency activity at its peak latencies, e.g., at 85 and 140 ms in Fig. 4B. It is also the high frequency activity that contributes to the MI results—it does survive when the MI maps are used to identify common links across subjects (Fig. 7). Using central (5.7 × 5.7°) presentation and the same 200 Hz for the upper filter cut in a recent MEG study, Liu et al. (2002) found a face-selective MEG response in posterior areas between 85 and 131 ms, close to the latencies we reported here about the FG activity (for central and peripheral presentation, at 80 and 70 ms, respectively), but in that study the authors did not localize generators of the early response, and only indicated that the source of this early component must be beyond retinotopic cortex. In the present study, we have identified an early response at similar latencies and localized it to the fusiform gyri.

Central vs. peripheral processing

To date, only a few neuroimaging studies have been carried out using faces presented in periphery. An fMRI study showed that activity in posterior FG area was significantly stronger in response to central stimuli compared to mid and peripheral stimuli (Levy et al., 2001). This result is confirmed by our present study: FG activity was significantly stronger for central than for peripheral presentation (Fig. 6, about 38% stronger). V1/V2 activity, however, was significantly stronger for lower than central and upper visual field stimulation (Fig. 5). The weaker activity elicited by centrally presented images may be due to the spread of activity over the lips of the calcarine operculum and the presence of radial components which produce no MEG signal. Furthermore, the present MEG study provides ROI activation time courses in a millisecond scale, which would not be possible with fMRI. Both the V1/V2 and FG onset latency (first peak latency) was shorter for peripheral than for central presentation (Figs. 5 and 6). The latency

difference reached a significant level for the FG activity but not for the V1/V2 activity.

We used mutual information analysis to examine whether connectivity patterns change systematically at the center and the four quadrants. For central presentation, the linkage was from V1/V2 to FG (Fig. 7A). Lower visual field presentation also showed a linkage from V1/V2 to FG, but this was soon followed by feedback connections from FG to V1/V2 (Fig. 7C). In comparison, for upper visual field presentation, the linkage was from FG to V1/V2, unidirectional for UL and bi-directional for UR presentation (Fig. 7C).

Differences among quadrant presentations

In the present study, using quadrant presentation and a larger offset from the center than previous studies, we were able to specify the spatial and temporal differences for images presented to different quadrants. Both the left vs. right and the upper vs. lower visual fields differ in striking way. The left and right visual fields are not associated with any a priori ecological differences because our environment does not impose pervasive differences in the types of information that we encounter on the left vs. right sides of space. The left and right visual fields, however, project to different cerebral hemispheres. Our current results (Figs. 5 and 6 and Tables 2 and 3) showed that both contralateral V1/V2 and FG ROI activities were earlier (about 10 and 23 ms earlier in V1/V2 and FG, respectively) and significantly stronger than their ipsilateral counterparts (about 57% and 32% stronger in V1/V2 and FG, respectively). This suggested that stimuli were processed predominantly in the directly stimulated (i.e., contralateral) hemisphere.

The upper and lower visual fields are strongly associated with far vs. near vision, respectively, giving rise to clear ecological differences in the types of information that are typically encountered in the upper vs. lower fields (Previc, 1990). The use of faces as an important instrument of emotional expression and other social communication is of particular importance to far vision (upper visual field). The lower visual field appears to have better spatial resolution compared with the upper visual field (Rubin et al., 1996). Our current result (Fig. 5 and Table 2) showed that the V1/V2 activity was significantly stronger for lower than for upper visual field stimulation (about 69% stronger). This result agrees with two recent MEG studies using checkerboards (Portin et al., 1999) and grating patterns (Tzelepi et al., 2001). These two studies also showed stronger occipital cortical activation to lower than upper visual field stimuli, which suggested that the lower visual field input may dominate in the early cortical responses to hemifield stimuli.

Furthermore, the upper and lower fields project to anatomically distinct regions (Maunsell and Newsome, 1987). The lower visual field and the dorsal system – V2, V3, V4, middle temporal cortex (MT), middle superior temporal cortex (MST) and posterior parietal cortex (area 7a) – are critically linked to the visual control of reaching and other manipulations in peripersonal visual space. Our results support this sequence of events showing a rapid spread of activity from V1/V2 to FG (Fig. 7C). Conversely, the upper visual field and the ventral system – V2, ventral posterior cortex (VP), V4 and inferotemporal cortex (IT) – are better suited to search for and recognize objects, including faces, in extra-personal space. Our results showed the linked activity from FG to V1/V2 for the upper visual field stimulation (Fig. 7C). A recent combined fMRI and ERP study (Vanni et al., 2004) reported that distinct visual patterns interacted first in the higher-order visual areas (e.g., lateral occipital V5 region) rather than in the lower-order areas (e.g., V1/V2/V3). This suggested that higher-order visual areas may be the first to pool spatial information across the whole visual field in the integrated model as proposed by Bullier (2001): information arriving in the cortex from the magnocellular layers of the lateral geniculate nucleus is first sent and processed in the parietal cortex and then sent back by feedback connections to areas V1 and V2 that act as 'active blackboards' for the rest of the visual cortical areas. Our results suggest that in addition to the strong magnocellular input in the dorsal system, a ventral magnocellular pathway is excited by face stimuli in the upper visual field.

Unresolved questions

Our study demonstrated that early processing of visual stimuli of different facial expressions of emotions in a face affect recognition task elicits early responses in V1/V2 and the FG that strongly depend on the presentation location in the visual field. Two important questions remain unresolved and they are the subject of ongoing studies. First, we used a block design for the stimulus presentation (i.e., stimuli were presented in the same part of the visual field within a recording run). It is possible that early responses would be facilitated by such a block presentation. Second, the face specificity of the activations we have identified. Adding runs with different objects would have increased the length of the MEG experiment beyond what was practical for MEG recording (usually a subject became tired after 4 h of recording). The present study is a follow-up of our earlier MEG studies on face processing using the same face stimuli in an object recognition and face affect recognition task (Liu et al., 1999; Ioannides et al., 2000, 2004). Although we recorded the MEG signal from different sets of subjects with different MEG systems, the identified FG ROI was comparable across our studies and similar to those that have been reported for face-selective responses by other fMRI studies (Kanwisher et al., 1997; Halgren et al., 1999) (Table 1). In our earlier studies, regions of highly significant changes in activity were identified in similar areas for each subject when the post-stimulus responses were contrasted with baseline activations and when responses to face stimuli were compared to responses from all other (nonface) stimuli (Ioannides, 2001). Here we recorded on one of the subjects from the current study using checkerboards instead of faces displayed in exactly the same way as in the face experiment. The fusiform activity for checkerboards as compared to faces was consistently weaker but had similar activation profile (Fig. 4D). This result for one subject together with a face-selective response at a latency of 100 ms (Liu et al., 2002) suggests that at least part of the early (within 100 ms) FG activations are face-specific, but firm confirmation must await the results of ongoing studies. We note, however, that the study of responses as they occur, i.e., without subtraction from a baseline condition as is possible with our methods, shows consistently that face specificity is a quantitative rather than a qualitative effect (Liu et al., 1999). We also showed that only for faces the processing was dominated by a feedforward link from V1/V2 (around 100 ms) and fusiform gyrus (around 150 ms). For other objects, this feed-forward link was absent, replaced by a feedback link from the same fusiform activation (around 150 ms) leading to a reactivation of V1/V2 some 50 to 100 ms later (Ioannides, 2001; Ioannides et al., 2000). The details for face activation were probed further in the present

study using smaller image sizes and presentations in different parts of the visual field to study whether regional activations and connectivity patterns change systematically in the fovea and the four quadrants. It thus appears that there is a gradient of face specificity in the fusiform response, much as one might have predicted from two recent studies (Haxby et al., 2001; Hanson et al., 2004).

Summary and outlook

In summary, we studied magnetoencephalographic responses from eight human subjects to centrally and peripherally presented faces. Using our tomographic and statistical parametric mapping analyses, we identified occipitotemporal areas activated by face stimuli more than by control conditions. Regional time courses and mutual information analyses demonstrated that the spatiotemporal dynamics and connectivity patterns for images presented to the center and one of the quadrants are different. For the V1/V2 activity, we found (1) significantly stronger for lower than central and upper visual field presentation, (2) earlier activation for peripheral than for central presentation and (3) in the periphery, contralateral V1/V2 activated about 10 ms earlier and significantly stronger than ipsilateral V1/V2. For the FG activity, we found (1) significantly stronger for central than for peripheral presentation, (2) significant earlier activation for peripheral than for central presentation, (3) in the periphery, contralateral FG activated significantly earlier (about 23 ms) and stronger than ipsilateral FG, and notably, (4) fast responses in the fusiform were seen at 70–80 ms after image onset, well before the latencies characteristic of the N170 and M170 which have often been attributed to the FG activation. As for the connectivity between V1/V2 and FG, we showed linked activity from V1/V2 to fusiform for central and lower visual field presentations. In the upper visual field, the linkage was from fusiform to V1/V2. Our results showed that face stimuli are processed predominantly in the hemisphere contralateral to the stimulation and demonstrated for the first time early fusiform activation leading V1/V2 activation for upper visual field stimulation.

In conclusion, our results support the hypothesis that how visual processing is initiated in the cortex depends very strongly on where it appears in the visual field, at least with faces as stimuli in a facial expression recognition task. It is left for future studies to qualify which of the details of early visual processing are specific to faces and the task we have used. It is also a task of future studies to show how the strong dependence of early visual processing on visual field presentation is almost erased by the time a behavioral response is made.

References

Allison, T., Ginter, H., Mccarthy, G., Nobre, A.C., Puce, A., Luby, M., Spencer, D.D., 1994. Face recognition in human extrastriate cortex. J. Neurophysiol. 71, 821–825.

Allison, T., Puce, A., Spencer, D.D., Mccarthy, G., 1999. Electrophysiological studies of human face perception: I. Potentials generated in occipitotemporal cortex by face and non-face stimuli. Cereb. Cortex 9, 415–430.

Bentin, S., Allison, T., Puce, A., Perez, E., Mccarthy, G., 1996. Electrophysiological studies of face perception in humans. J. Cogn. Neurosci. 8, 551–565.

Bullier, J., 2001. Integrated model of visual processing. Brain Res. Rev. 36, 96–107.

Damasio, A.R., Tranel, D., Damasio, H., 1990. Face agnosia and the neural substrates of memory. Annu. Rev. Neurosci. 13, 89–109.

Eimer, M., 1998. Does the face-specific N170 component reflect the activity of a specialized eye processor? NeuroReport 9, 2945–2948.

Ekman, P., Friesen, W.V., 1976. Pictures of Facial Affect. Consulting Psychologists Press, Palo Alto, CA.

Gauthier, I., Tarr, M.J., Moylan, J., Skudlarski, P., Gore, J.C., Anderson, A.W., 2000. The fusiform "face area" is part of a network that processes faces at the individual level. J. Cogn. Neurosci. 12, 495–504.

George, N., Evans, J., Fiori, N., Davidoff, J., Renault, B., 1996. Brain events related to normal and moderately scrambled faces. Cogn. Brain Res. 4, 65–76.

Gross, J., Ioannides, A.A., 1999. Linear transformations of data space in MEG. Phys. Med. Biol. 44, 2081–2097.

Halgren, E., Dale, A.M., Sereno, M.I., Tootell, R.B.H., Marinkovic, K., Rosen, B.R., 1999. Location of human face-selective cortex with respect to retinotopic areas. Hum. Brain Mapp. 7, 29–37.

Halgren, E., Raij, T., Marinkovic, K., Jousmaki, V., Hari, R., 2000. Cognitive response profile of the human fusiform face area as determined by MEG. Cereb. Cortex 10, 69–81.

Hanson, S.J., Matsuka, T., Haxby, J.V., 2004. Combinatorial codes in ventral temporal lobe for object recognition: Haxby (2001) revisited: is there a "face" area? NeuroImage 23, 156–166.

Haxby, J.V., Horwitz, B., Ungerleider, L.G., Maisog, J.M., Pietrini, P., Grady, C.L., 1994. The functional-organization of human extrastriate cortex—A PET-rCBF study of selective attention to faces and locations. J. Neurosci. 14, 6336–6353.

Haxby, J.V., Gobbini, M.I., Furey, M.L., Ishai, A., Schouten, J.L., Pietrini, P., 2001. Distributed and overlapping representations of faces and objects in ventral temporal cortex. Science 293, 2425–2430.

Hironaga, N., Schellens, M., Ioannides, A.A., 2002. Accurate co-registration for MEG reconstructions. In: Nowak, H., Hueisen, J., GieBler, F., Huonker, R. (Eds.), Proceedings of the 13th International Conference on Biomagnetism. VDE Verlag, Berlin, pp. 931–933.

Ioannides, A.A., 2001. Real time human brain function: observations and inferences from single trial analysis of magnetoencephalographic signals. Clin. Electroencephalogr. 32, 98–111.

Ioannides, A.A., Bolton, J.P.R., Clarke, C.J.S., 1990. Continuous probabilistic solutions to the biomagnetic inverse problem. Inverse Problems 6, 523–542.

Ioannides, A.A., Liu, M.J., Liu, L.C., Bamidis, P.D., Hellstrand, E., Stephan, K.M., 1995. Magnetic field tomography of cortical and deep processes: examples of "real-time mapping" of averaged and single trial MEG signals. Int. J. Psychophysiol. 20, 161–175.

Ioannides, A.A., Liu, L.C., Kwapien, J., Drozdz, S., Streit, M., 2000. Coupling of regional activations in a human brain during an object and face affect recognition task. Hum. Brain Mapp. 11, 77–92.

Ioannides, A.A., Poghosyan, V., Dammers, J., Streit, M., 2004. Real-time neural activity and connectivity in healthy individuals and schizophrenia patients. NeuroImage 23, 473–482.

Ioannides, A.A., Fenwick, P.B., Liu, L., 2005. Widely distributed magnetoencephalography spikes related to the planning and execution of human saccades. J. Neurosci. 25, 7950–7967.

Itier, R.J., Taylor, M.J., 2004. N170 or N1? Spatiotemporal differences between object and face processing using ERPs. Cereb. Cortex 14, 132–142.

Jahn, O., Cichocki, A., Ioannides, A.A., Amari, S., 1999. Identification and elimination of artifacts from MEG signals using extended independent component analysis. In: Yoshimoto, T., Kotani, M., Kuriki, S., Karibe, H., Nakasato, N. (Eds.), Recent Advances in Biomagnetism. Tohoku Univ. Press, Sendai, pp. 224–228.

Kanwisher, N., McDermott, J., Chun, M.M., 1997. The fusiform face area: a module in human extrastriate cortex specialized for face perception. J. Neurosci. 17, 4302–4311.

Levy, I., Hasson, U., Avidan, G., Hendler, T., Malach, R., 2001. Center-periphery organization of human object areas. Nat. Neurosci. 4, 533–539.

Linkenkaer-Hansen, K., Palva, J.M., Sams, M., Hietanen, J.K., Aronen, H.J., Ilmoniemi, R.J., 1998. Face-selective processing in human extrastriate cortex around 120(ms after stimulus onset revealed by magneto- and electroencephalography. Neurosci. Lett. 253, 147–150.

Liu, L.C., Ioannides, A.A., Streit, M., 1999. Single trial analysis of neurophysiological correlates of the recognition of complex objects and facial expressions of emotion. Brain Topogr. 11, 291–303.

Liu, J., Harris, A., Kanwisher, N., 2002. Stages of processing in face perception: an MEG study. Nat. Neurosci. 5, 910–916.

Lyons, M.J., Akamatsu, S., Kamachi, M., Gyoba, J., 1998. Coding facial expressions with gabor wavelets. Third IEEE International Conference on Automatic Face and Gesture Recognition. IEEE Computer Society, Nara, Japan, pp. 200–205.

Maunsell, J.H.R., Newsome, W.T., 1987. Visual processing in monkey extrastriate cortex. Annu. Rev. Neurosci. 10, 363–401.

McCarthy, G., Puce, A., Gore, J.C., Allison, T., 1997. Face-specific processing in the human fusiform gyrus. J. Cogn. Neurosci. 9, 605–610.

McCarthy, G., Puce, A., Belger, A., Allison, T., 1999. Electrophysiological studies of human face perception: II. Response properties of face-specific potentials generated in occipitotemporal cortex. Cereb. Cortex 9, 431–444.

Meadows, J.C., 1974. Anatomical basis of prosopagnosia. J. Neurol. Neurosurg. Psychiatry 37, 489–501.

Melmoth, D.R., Kukkonen, H.T., Makela, P.K., Rovamo, J.M., 2000. The effect of contrast and size scaling on face perception in foveal and extrafoveal vision. Investig. Ophthalmol. Vis. Sci. 41, 2811–2819.

Moradi, F., Liu, L.C., Cheng, K., Waggoner, R.A., Tanaka, K., Ioannides, A.A., 2003. Consistent and precise localization of brain activity in human primary visual cortex by MEG and fMRI. NeuroImage 18, 595–609.

Noesselt, T., Driver, J., Heinze, H.J., Dolan, R., 2005. Asymmetrical activation in the human brain during processing of fearful faces. Curr. Biol. 15, 424–429.

Portin, K., Vanni, S., Virsu, V., Hari, R., 1999. Stronger occipital cortical activation to lower than upper visual field stimuli—Neuromagnetic recordings. Exp. Brain Res. 124, 287–294.

Previc, F.H., 1990. Functional specialization in the lower and upper visual-fields in humans—Its ecological origins and neurophysiological implications. Behav. Brain Sci. 13, 519–541.

Puce, A., Allison, T., Gore, J.C., Mccarthy, G., 1995. Face-sensitive regions in human extrastriate cortex studied by functional MRI. J. Neurophysiol. 74, 1192–1199.

Rovamo, J., Makela, P., Nasanen, R., Whitaker, D., 1997. Detection of geometric image distortions at various eccentricities. Invest. Ophthalmol. Visual Sci. 38, 1029–1039.

Rubin, N., Nakayama, K., Shapley, R., 1996. Enhanced perception of illusory contours in the lower versus upper visual hemifields. Science 271, 651–653.

Sergent, J., Poncet, M., 1990. From covert to overt recognition of faces in a prosopagnosic patient. Brain 113, 989–1004.

Sergent, J., Ohta, S., Macdonald, B., 1992. Functional neuroanatomy of face and object processing—A positron emission tomography study. Brain 115, 15–36.

Streit, M., Ioannides, A.A., Liu, L., Wolwer, W., Dammers, J., Gross, J., Gaebel, W., Muller-Gartner, H.W., 1999. Neurophysiological correlates of the recognition of facial expressions of emotion as revealed by magnetoencephalography. Brain Res. Cogn Brain Res. 7, 481–491.

Streit, M., Ioannides, A., Sinnemann, T., Wolwer, W., Dammers, J., Zilles, K., Gaebel, W., 2001. Disturbed facial affect recognition in patients with schizophrenia associated with hypoactivity in distributed brain regions: a magnetoencephalographic study. Am. J. Psychiatry 158, 1429–1436.

Streit, M., Dammers, J., Simsek-Kraues, S., Brinkmeyer, J., Wolwer, W., Ioannides, A., 2003. Time course of regional brain activations during facial emotion recognition in humans. Neurosci. Lett. 342, 101–104.

Talairach, J., Tournoux, P., 1988. Co-planar Stereotaxic Atlas of the Human Brain. Thieme, New York.

Taylor, J.G., Ioannides, A.A., Muller-Gartner, H.W., 1999. Mathematical analysis of lead field expansions. IEEE Trans. Med. Imag. 18, 151–163.

Terasaki, O., Okazaki, M., 2002. Transcallosal conduction time measured by visual hemifield stimulation with face images. NeuroReport 13, 97–99.

Tzelepi, A., Ioannides, A.A., Poghosyan, V., 2001. Early (N70m) neuromagnetic signal topography and striate and extrastriate generators following pattern onset quadrant stimulation. NeuroImage 13, 702–718.

Vanni, S., Dojat, M., Warnking, J., Delon-Martin, C., Segebarth, C., Bullier, J., 2004. Timing of interactions across the visual field in the human cortex. NeuroImage 21, 818–828.

Watanabe, S., Kakigi, R., Puce, A., 2003. The spatiotemporal dynamics of the face inversion effect: a magneto- and electro-encephalographic study. Neuroscience 116, 879–895.